

Electrical and optical properties of self-assembled InAs quantum dots in InP studied by space-charge spectroscopy and photoluminescence

H. Pettersson, C. Pryor, L. Landin, M.-E. Pistol, N. Carlsson, W. Seifert, and L. Samuelson

Solid State Physics, Lund University, Box 118, S-221 00 Lund, Sweden

(Received 16 April 1998; revised manuscript received 16 August 1999)

In this paper, we report on a detailed investigation using junction space-charge techniques and photoluminescence of InAs quantum dots embedded in an InP matrix. From measurements of thermal emission rates we have determined the ground-state energy of electrons and holes bound to the InAs dots. In contrast to other dot systems the holes are found to be more strongly confined than the electrons. Corresponding optical emission rates have been measured for holes and the photoionization is found to be well described by a photothermal excitation process similar to what has previously been observed for deep impurities. Furthermore, we have performed photoluminescence measurements revealing excited hole states with energies in good agreement with theory.

I. INTRODUCTION

During the past years, a lot of attention has been devoted to the growth and characterization of self-assembled quantum dots (SAD's).^{1,2} The strong interest in these systems is readily understood in view of their obvious potential for future high-speed electronic devices as well as for their intriguing physical properties.

So far, most studies have focused on InAs SAD's in GaAs (Refs. 3–5) and InP SAD's in GaInP.^{6–8} Considerably less attention has been given to InAs SAD's in InP. In fact, very little is known about their electronic properties. In view of the strong luminescence of these dots⁹ at about 1.55 μm , which makes them well suited for optoelectronic communication devices, e.g., lasers with a low threshold current, high modulation speed, and temperature insensitivity,¹⁰ a detailed understanding of their electronic properties is of great interest.

In this paper, we report on the results of the first detailed investigation of these dots using junction space charge techniques (JSCT's) including deep level transient spectroscopy (DLTS) (Ref. 11) and photocapacitance spectroscopy,¹² as well as photoluminescence spectroscopy. In particular, we have determined an unusually large valence band offset of about 460 meV which suggests that these quantum dots may also be used for memory applications. This large valence band offset is supported by theoretical calculations.

II. EXPERIMENTAL DETAILS

The samples used were grown by metalorganic vapor phase deposition on n^+ InP substrates. The InAs dots are situated in between two 2 μm thick epitaxial InP layers with a residual doping concentration of about 10^{15} cm^{-3} . The details of the growth are discussed elsewhere.¹³ The InAs SAD's are randomly distributed with a density of $2 \times 10^{10} \text{ cm}^{-2}$ and their typical dimensions are 6 nm in height and 35 by 45 nm in base determined from AFM measurements. Schottky junctions were formed by defining semi-transparent Au contacts on the top InP layer and alloyed Au-Ge ohmic contacts on the InP substrate.

The DLTS measurements were performed using a commercial DLS83 spectrometer from SemiLab, Hungary. For the photocapacitance measurements we employed a 0.5 m grating monochromator from Acton Research and a Boonton capacitance meter. In PL the 488 nm line from an Ar-ion laser was used as the excitation source and the spectra were collected using a LN₂ cooled Ge detector.

III. MEASUREMENTS EMPLOYING JSCT's

A. Thermal emission rates and the binding energy of electrons

JSCT's has turned out to be a powerful experimental approach to determining electronic properties, e.g., thermal emission rates and binding energies of deep levels in semiconductors.¹² Quite recently, these techniques have also been invoked in the study of SAD's.^{5,7,8,14} To determine the binding energy of electrons bound to the InAs quantum dots, we measured thermal emission rates at different temperatures using DLTS. Figure 1 shows the DLTS signal obtained at different filling pulse biases while keeping the detection bias at a constant value of -2.5 V . The detection bias was cho-

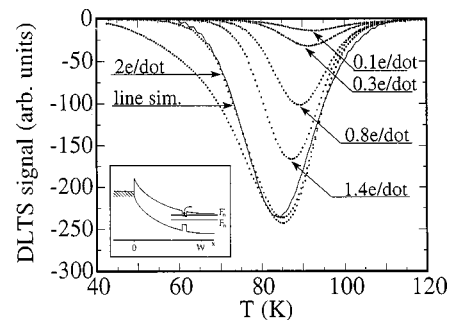


FIG. 1. DLTS spectra obtained at increasing filling pulse biases corresponding to an average occupancy of about 0.1 electron/dot to 2 electrons/dot. The full line represents a simulated spectrum in the case of 2 electrons/dot. The inset shows schematically the energy band diagram with the position of the Fermi level at the detection bias, F_n , and at a filling pulse bias where electrons are injected into the dots, F_n' .

sen so that the quantum dots are within the depletion region of the Schottky contact. The DLTS peak amplitude is proportional to the amount of charge trapped by the SAD's, whereas the peak position is related to the thermal emission rate of the trapped electrons (for details on DLTS see Ref. 11). We note that by increasing the filling pulse bias (see insert of Fig. 1) the peak amplitude increases to a certain saturation value. The reason for the increase in peak amplitude with increased bias is twofold. First, the number of electrons per dot increases and, second, since the dots are distributed in energy due to differences in strain and size, we successively probe a larger part of the distribution of dots. The corresponding average electron occupancy in each dot can be determined from the sheet concentration of SAD's, n_{dot} , and the relative DLTS peak amplitude $\Delta C/C$ using the expression

$$\Delta C/C = n_{\text{dot}}L/(W^2N_D), \quad (1)$$

where L is the distance from the dot plane to the surface, W is the width of the depletion region, and N_D is the doping density in the InP barriers. Using the saturation value of the DLTS peak and the concentration of dots measured by AFM ($2 \times 10^{10} \text{ cm}^{-2}$ within an accuracy of 20%) we estimate an average occupancy of 2 electrons/dot, with these bias conditions. Since the ground state of the dots is expected to be twofold degenerate we conclude that the saturated DLTS peak corresponds to a full groundstate of the ensemble of dots. Furthermore, we observe that the peak position changes towards lower temperatures when we increase the filling pulse bias. This is due to the above-mentioned inhomogeneous broadening of the ground state as well as the induced broadening due to electron-electron interactions between the two electrons in the ground state (Coulomb charging effects). The full curve in Fig. 1 (marked by "line sim.") shows the result of a simulation of the expected shape of the DLTS peak for the case of 2 electrons per dot under the assumption of a Gaussian distributed ground-state energy ΔE_e with a FWHM of about 25 meV. Increasing the filling pulse bias beyond the point of saturation results in a slight increase of the DLTS peak at the low temperature side. The origin of this effect is not fully understood, but it probably reflects the presence of excited states in the dots. This conclusion is supported by theory as well as by more recent absorption measurements which indeed reveal excited states at about 50 meV above the ground state.

By performing repetitive DLTS scans for different detection frequencies we measured the thermal emission rates e_e^t at different temperatures. In the case of a deep trap the correlation between thermal emission rates and the binding energy ΔE_e of the electrons can easily be worked out from the detailed balance between thermal emission and thermal capture rates of electrons. In the case of quantum dots such an approach is complicated by the presence of many excited states from which carrier emission and capture processes can take place. Following arguments from calculations made for deep traps with excited states¹⁵ we propose that the emission of the trapped electrons predominantly takes place via excited states located close to (within some kT) the conduction band of the InP barrier. This is a reasonable model considering that the SAD's are grown on a wetting layer which provides a large number of states close to the band edge.

The thermal emission rate from the groundstate to such an excited state $e_{g \rightarrow e}^t$ is given by

$$e_{g \rightarrow e}^t(T) = g_e/g_g r_{e \rightarrow g}^t \exp[(-\Delta E_{g,e})/kT], \quad (2)$$

where g_e/g_g is the degeneracy ratio between the excited state and the ground state, $r_{e \rightarrow g}^t$ is the recombination rate from the excited state to the ground state, and $\Delta E_{g,e}$ is the energy separation between the excited state and the ground state. Similarly, the thermal emission rate from the excited state to the conduction band $e_{e \rightarrow \text{CB}}^t$, is given by

$$e_{e \rightarrow \text{CB}}^t(T) = 1/g_e \sigma_0^t \langle v_{\text{th}} \rangle N_c \exp(-\Delta E_{e,\text{CB}}/kT), \quad (3)$$

where σ_0^t is the capture cross section related to the scattering of electrons into the excited state, $\langle v_{\text{th}} \rangle$ is the thermal velocity, N_c is the effective density of states in the conduction band, and $\Delta E_{e,\text{CB}}$ is the energy depth of the excited state from the conduction band. The resulting thermal emission rate for the ionization process can be shown to be given by

$$e_{g \rightarrow \text{CB}}^t = e_{g \rightarrow e}^t e_{e \rightarrow \text{CB}}^t / (r_{e \rightarrow g}^t + e_{e \rightarrow \text{CB}}^t). \quad (4)$$

At temperatures low enough so that $r_{e \rightarrow g}^t > e_{e \rightarrow \text{CB}}^t$ Eq. (4) reduces to

$$e_{g \rightarrow \text{CB}}^t(T) = 1/g_g \sigma_0^t \langle v_{\text{th}} \rangle N_c \exp(-\Delta E_{g,\text{CB}}/kT), \quad (5)$$

where $\Delta E_{g,\text{CB}}$ is the energy depth of the ground state from the conduction band. At higher temperatures where instead $e_{e \rightarrow \text{CB}}^t > r_{e \rightarrow g}^t$ Eq. (4) reduces to

$$e_{g \rightarrow \text{CB}}^t(T) = e_{g \rightarrow e}^t(T) = g_e/g_g r_{e \rightarrow g}^t \exp[(-\Delta E_{g,e})/kT]. \quad (6)$$

Since the states in the wetting layer are continuous in energy we argue that some suitable excited state will exist which makes Eq. (6) valid. From Eq. (6) it is thus evident that the binding energy we would obtain by plotting the measured thermal emission rates in an Arrhenius plot is the separation between an excited state close to the conduction band and the ground state. Here we have neglected the temperature dependence of $r_{e \rightarrow g}^t$ which is a reasonable assumption. Figure 2 shows an Arrhenius plot of the thermal emission rates measured at different detection frequencies at high (saturated) and low electron occupancy. From the slopes of the straight lines we obtain binding energies of 175 meV and 190 meV, respectively. The difference reflects the broadening of the DLT'S peak discussed above. At low occupancy we deduce a slightly larger activation energy since we then probe an energetically lower part of the distribution of dots and in addition the Coulomb charging effect is negligible. It might be argued that the slope of the curve corresponding to high electron concentration should not be a constant. However, since the total broadening is only about 25 meV we do not observe any variation in the slope.

Due to the fact that these measurements are performed in the presence of a high electric field (of the order of 10^4 V/cm – 10^5 V/cm) the emission barrier which the trapped electrons have to surmount is reduced. By measuring the activation energy at different detection biases an approximate linear relationship between activation energy and electric field was found which is qualitatively in agreement with Ref. 16. Extrapolation to zero field yields an activation en-

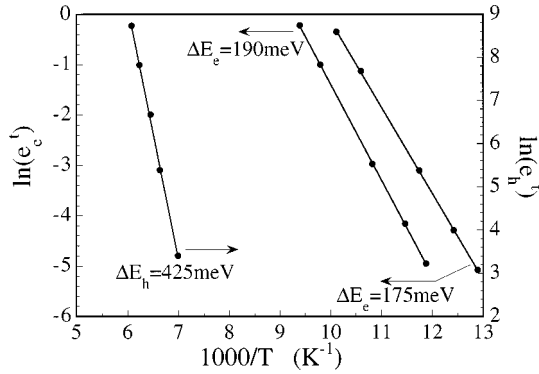


FIG. 2. Arrhenius plot of the thermal emission rates for electrons e_e^- and holes e_h^- , respectively, with indicated ground-state energies. The difference between the two shown ground-state energies for electrons ΔE_e is discussed in Sec. III A.

ergy of about 190 meV (for the case of saturation). In this context it should also be mentioned that due to the high electric field a pure tunneling or phonon assisted tunneling process from the excited state into the conduction band is also plausible which obviously implies that the true binding energy is slightly larger than 190 meV.

It should also be mentioned that we have tried to measure the capture rate of electrons into the SAD's. Such measurements would give information about the energy position of the excited state.¹⁵ Capture rates are normally measured in a DLTS experiment where the duration of the filling pulse is varied. For the InAs dots it was, however, not possible to measure the capture rates simply because the rate was too large. DLTS peaks recorded at, e.g., pulse lengths of 50 ns and 1 ms were basically identical. A fast capture is of advantage for many photonic applications.

B. Thermal emission rates and the binding energy of holes

In order to measure the corresponding thermal emission rate of holes e_h^- using DLTS, holes must be injected into the dots during the filling pulse. Since the material in our case is n type this is obviously not possible. Instead we invoked a single-shot capacitance transient technique¹² where the initial hole occupancy was realized using illumination with photons having energies of about 1.2 eV. In this process electron-hole pairs are created in the dots. The electrons subsequently escape from the dots at a faster rate than holes due to, e.g., black-body radiation (very effective light source at photon energies of about 200 meV) resulting in a net accumulation of holes in the dots. Following this filling procedure the light source was removed and the thermal reemission of the trapped holes was studied. It should be pointed out that this technique is not a repetitive technique such as the DLTS, but rather one extracts the emission rate directly from single capacitance transients given by

$$\Delta C(t, T) = \Delta C_\infty \{1 - \exp[-e_h^-(T) \cdot t]\}, \quad (7)$$

where ΔC_∞ is the total change in capacitance due to the positively charged dots [analogous to ΔC in Eq. (1)] and e_h^- is the thermal emission rate of holes. By measuring such capacitance transients at different temperatures it is thus possible to determine the temperature dependence of the thermal

emission rate. The correlation between e_h^- and the binding energy of holes ΔE_h is given by an expression analogous to Eq. (6). The Arrhenius plot in Fig. 2 includes thermal emission rates of holes from which an activation energy of about 425 meV could be deduced. After correction for the field induced barrier lowering as discussed previously we find a ground-state energy of holes of about 440 meV.

C. Optical emission rates of holes

Following the determination of ground-state energies for electrons and holes from measurements of thermal emission rates, we proceeded to studying the corresponding optical emission rates. Optical emission rates have been studied in numerous papers on deep impurity levels (see, e.g., Ref. 17). From such measurements one can in general draw conclusions about, e.g., the binding energy of charge carriers, the type of the binding potential and details about the emission process, e.g., if excited states close to the conduction band are involved. Also, it is important to compare binding energies obtained from electrical and optical measurements. From studies of deep traps it is well known that large discrepancies might exist. As an example we would like to mention the DX center where the thermal and optical binding energies differ by about 700 meV due to a large Franck-Condon shift.¹⁸

In our case, since the ground-state energy for electrons is quite small any trapped electrons will, as already pointed out, be emitted due to, e.g., black body radiation within a few seconds. Since typical optical emission rates due to monochromatic illumination from a normal tungsten lamp yields optical emission rates lower than 1 s^{-1} we were not able to measure the optical emission rate of electrons. In contrast, due to the large binding energy of holes we could study the optical emission rate of holes e_h^0 over several orders of magnitude. To be able to do so, an initial accumulation of holes was produced in the dots in the same way as discussed in Sec. III B. Following this optical filling pulse we removed this light source and illuminated the sample with a secondary light source from which we obtained tuneable monochromatic light. This illumination resulted in capacitance transients given by

$$\Delta C(t, h\nu) = \Delta C_\infty \{1 - \exp[-e_h^0(h\nu) \cdot t]\}. \quad (8)$$

From analyses of such capacitance transients recorded at different photon energies the spectral distribution of the optical emission rate of holes e_h^0 could be determined. In addition, we performed these measurements at different temperatures (keeping the temperature low enough to avoid thermal emission). The optical emission rate is related to the photoionization cross-section σ_h^0 , via

$$e_h^0(h\nu) = \Phi(h\nu) \cdot \sigma_h^0(h\nu), \quad (9)$$

where $\Phi(h\nu)$ is the photon flux. Figure 3 shows the spectral distribution of the photoionization cross section σ_h^0 obtained at four different temperatures. From this plot it is evident that σ_h^0 varies nearly exponentially over more than two orders of magnitude. Interestingly, we note that if we take into account the temperature dependence of the spectral distributions we

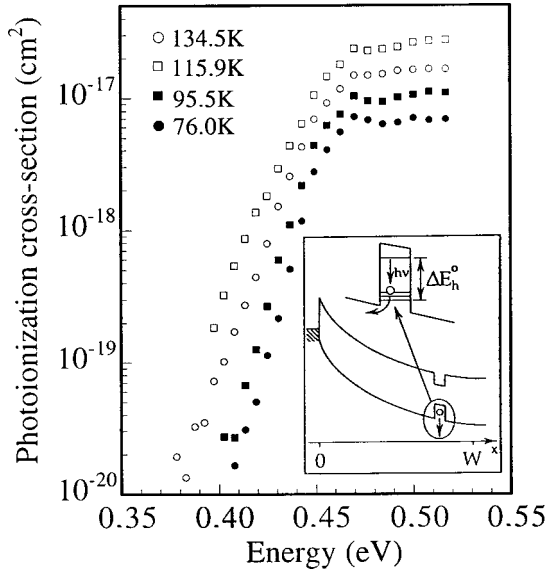


FIG. 3. Spectral distribution of the photoionization cross section of holes at four different temperatures. The inset shows schematically the proposed photothermal ionization model.

find that all the data in the exponential parts can be nicely fitted with one simple expression of type

$$P_{ex}(h\nu, T) = A \exp[-(h\nu - \Delta E_h^0)/k \cdot T]. \quad (10)$$

We explain this result by proposing an ionization process where bound holes are initially optically excited into a series of excited states close to the valence band of the barrier (such as states arising from the wetting layer) from which they are thermally ionized into the valence band. Such a composite ionization process has frequently been observed for deep levels. It is actually used as a spectroscopic technique referred to as photothermal ionization spectroscopy (PTIS) for studying excited states in deep levels. To the best of our knowledge this kind of excitation process has never before been observed for quantum dots. A simultaneous fitting of the experimental data in Fig. 3 results in a value of A of $1.0 \times 10^{-17} \text{ cm}^2$ and a binding energy ΔE_h^0 of 445 meV in excellent agreement with the value of 440 meV obtained from the measurement of thermal emission rates. This agreement lends further support to the model used for interpreting the experimental data.

IV. PHOTOLUMINESCENCE MEASUREMENTS

In Fig. 4 we show the spectral distribution of the PL signal both at low temperature (5 K) and at room temperature. The peak corresponding to luminescence from the ground state occurs at an energy of about 737 meV at a temperature of 5 K. This value corresponds to the recombination energy of an electron-hole pair, including the exciton binding energy. At 5 K we also observe the emission from the wetting layer at an energy of 1.225 eV.

By subtracting the single-particle energies obtained from the electrical measurements (Sec. III) from the bandgap of InP we deduce an energy of about 790 meV. The energy difference compared to the luminescence from the exciton

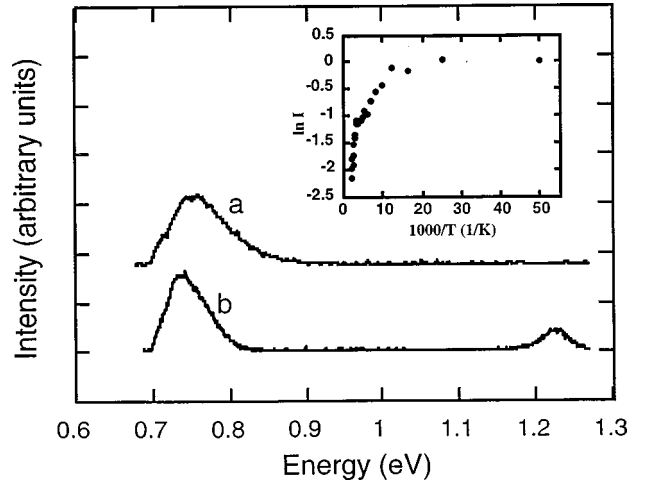


FIG. 4. PL spectra at different temperatures where trace (a) corresponds to 293 K and trace (b) to 5 K. In the inset we show the intensity dependence as a function of temperature.

ground state emission thus amounts to about 53 meV. This energy includes the exciton binding energy of about 20 meV (see Sec. V) and the energy difference between the excited states and the conduction and valence band, of the barrier respectively, discussed in Sec. III. Room-temperature PL shows emission only from the InAs quantum dots. The intensity decreases about three times between 5 K and room temperature. Although the emission energy is somewhat below 800 meV (corresponding to the technically important wavelength of $1.55 \mu\text{m}$), it is encouraging that the PL from the quantum dots is completely dominating the spectrum, pointing the way towards using this material system for a quantum dot laser in a commercially important wavelength range. It has been predicted that quantum dot lasers have important advantages over quantum well lasers, such as a reduced threshold current and a lower temperature sensitivity.¹⁰ It will be necessary to increase the confinement energy slightly using smaller InAs dots to reach an emission wavelength of $1.55 \mu\text{m}$. Recent progress in crystal growth has shown that it is possible to affect quantum dot sizes by varying the deposition rate or the deposition temperature.¹⁹ Figure 5 shows PL for different excitation power densities. A clear blueshift of the PL peak is observed as we increase the excitation power density, which we attribute to state filling⁶ of excited states. Assuming an inhomogeneous broadening of about 40–50 meV, a good agreement is observed between the experimentally obtained spectral distribution and a simulated spectrum from a series of excited states separated by about 20 meV. The calculations described below do indeed give a separation of excited hole states of about 20 meV.

V. THEORETICAL SIMULATIONS

The single-particle energies were calculated using an eight-band strain-dependent kp model, including the piezoelectric polarization resulting from the strain. The calculational technique is described in Ref. 20 where it was used to compute the electronic structure of InAs islands embedded in GaAs. One slight difference between this work and that in Ref. 20 is that it was necessary to add a term proportional to

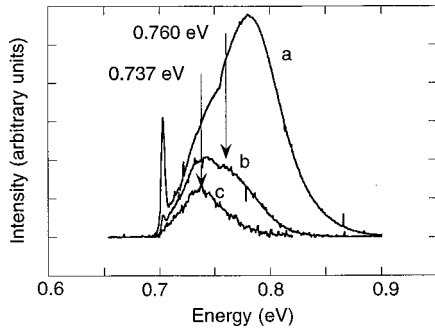


FIG. 5. PL spectra of the InAs quantum dots at different excitation power densities. The emission line having an energy of about 0.7 eV is an artifact arising from a band-gap related emission observed in second order (thus having a true emission energy of 1.4 eV).

k^4 . In an eight-band kp Hamiltonian it is possible that the dispersion relation crosses the gap at large momenta. This is, of course, an unphysical artifact since the Hamiltonian is invalid at large momenta anyway. Hence, the problem may be solved by adding a term proportional to k^4 which suppresses the unphysical modes. The material parameters for InP and InAs are given in Table I. The one required material parameter which is not directly tabulated is the band alignment between the InP and InAs. Since strain affects the band alignment as well, we are referring here to the contribution to the band offset which is independent of strain. We have treated the strain-independent offset as a fitting parameter,

TABLE I. Material parameters. Unless otherwise noted, values are taken from Ref. 26. The γ 's are the standard (as opposed to the modified) Luttinger parameters, E_g is the band-gap, Δ is the spin-orbit splitting, E_p is the Kane matrix element, a_g , a_c , a_v , b , and d are deformation potentials, e_{14} is the piezoelectric constant, ϵ_R is the relative dielectric constant, the C 's are the elastic constants, and a is the lattice constant.

Parameter	InAs	InP
γ_1	19.67	4.95
γ_2	8.37	1.65
γ_3	9.29	2.35
E_g	0.418 eV	1.424 eV
Δ	0.38 eV	0.11 eV
E_p	22.2 eV	20.4 eV
a_g	-6.0 eV	-6.6 eV
a_c	-6.66 eV	-7.0 eV ^a
a_v	0.66 eV	0.4 eV
b	-1.8 eV	-2.0 eV
d	-3.6 eV	-5.0 eV
e_{14}	0.045 C/m ² ^b	0.035 C/m ² ^b
ϵ_R	15.15	12.61
C_{xxxx}	8.329×10^{11} dyn/cm ²	10.22×10^{11} dyn/cm ²
C_{xyxy}	4.526×10^{11} dyn/cm ²	5.76×10^{11} dyn/cm ²
C_{xyxy}	3.959×10^{11} dyn/cm ²	4.6×10^{11} dyn/cm ²
a	0.60583 nm	0.58687 nm

^aReference 27.

^bReference 28.

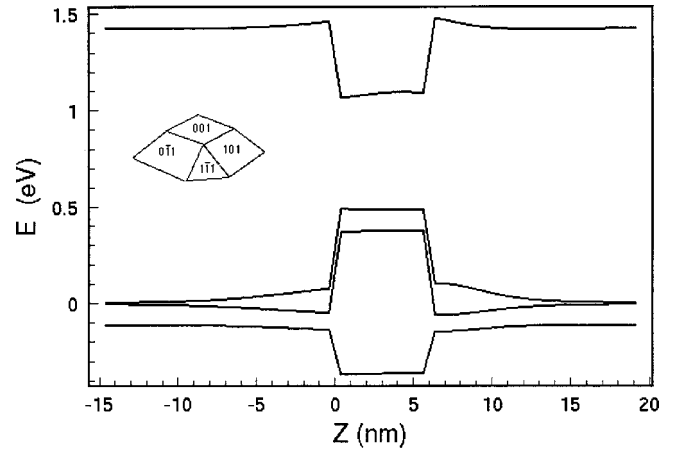


FIG. 6. A plot of the potential diagram of the InAs quantum dots in the z direction.

and find that an unstrained valence band offset of 0.40 eV fits the experimental data best. This value is in good agreement with a predicted value of 0.46 eV, based on the ‘‘model-solid’’ theory.²¹ After inclusion of strain, we get a valence band offset of 0.46 eV. Previous investigations using x-ray photoemission spectroscopy have found an unstrained valence band offset of 0.31 eV,²² whereas values of 0.27 eV (Ref. 23) as well as 0.41 eV (Ref. 24) have been found by photoluminescence spectroscopy on InAs quantum wells in InP. Due to the uncertainty in the determination of the geometry of the dots as well as the unknown degree of intermixing, our value for the valence band offset should be treated with some caution.

Figure 6 shows the potential profile along the growth axis, including an inset showing the shape of the dot used in the calculations. The dot height was 6 nm and the maximum elongation of the dot at the base was 14 nm. The potential depth is roughly equal for electrons and holes, about 0.5 eV. The calculated ground-state energies for the electrons and holes are 1.232 eV and 0.428 eV, respectively, where the zero is taken to be the top of the InP valence band, as in Fig. 6. These values correspond to binding energies of 0.192 eV for electrons and 0.428 eV for holes, which should be compared with the experimental values of 0.190 eV and 0.445 eV, respectively. We thus conclude that our theoretical model is adequate to describe highly strained quantum dots with strong confinement. The calculated separation between the first excited electron state and the ground-state energy is 70 meV and the corresponding separation for holes is 24 meV. We have also calculated the exciton binding energy for our quantum dots and find a value of 23 meV.

VI. SUMMARY AND DISCUSSION

In conclusion, we have reported on a comprehensive study of the electronic properties of self-organized InAs quantum dots embedded in InP, using both electrical and optical techniques. The data are mutually consistent and agree well with theoretical calculations. In contrast to most

systems we find that the depth of the valence band well is larger than that of the conduction band well. The binding energy of the holes is about 440 meV which is unusually large, also compared with room temperature (about 25 meV). For memory applications using charge storage in quantum dots,²⁵ it is advantageous if the charge carriers are not too

quickly thermally excited out of the dots. This system might thus be suitable for such devices.

ACKNOWLEDGMENT

This work was performed within the Nanometer Structure Consortium and was supported by NFR, TFR, and SSF.

-
- ¹P. M. Petroff and S. P. DenBaars, *Superlattices Microstruct.* **15**, 15 (1994).
- ²Y. Nabetani, T. Ishikawa, S. Noda, and A. Sasaki, *J. Appl. Phys.* **76**, 347 (1994).
- ³H. Drexler, D. Leonard, W. Hansen, J. P. Kotthaus, and P. M. Petroff, *Phys. Rev. Lett.* **73**, 2252 (1994).
- ⁴M. Grundman, J. Christen, N. N. Ledentsov, J. Bohrer, D. Bimberg, S. S. Ruvimov, P. Werner, U. Richter, U. Gosele, J. Heydenreich, V. M. Ustinov, A. Y. Egorov, A. E. Zhukov, P. S. Kopev, and Zh. I. Alferov, *Phys. Rev. Lett.* **74**, 4043 (1995).
- ⁵P. N. Brounkov, A. Polimeni, S. T. Stoddart, M. Henini, L. Eaves, P. C. Main, A. R. Kovsh, Y. G. Musikhin, and S. G. Konnikov, *Appl. Phys. Lett.* **73**, 1092 (1998).
- ⁶P. Castrillo, D. Hessman, M.-E. Pistol, S. Anand, N. Carlsson, W. Seifert, and L. Samuelson, *Appl. Phys. Lett.* **67**, 1905 (1995).
- ⁷S. Anand, N. Carlsson, M.-E. Pistol, L. Samuelson, W. Seifert, and L. R. Wallenberg, *Appl. Phys. Lett.* **67**, 3016 (1995).
- ⁸H. Pettersson, S. Anand, H. G. Grimmeiss, and L. Samuelson, *Phys. Rev. B* **53**, R10 497 (1996).
- ⁹H. Marchand, P. Desjardins, S. Guillon, J.-E. Paultre, Z. Bougrioua, R. Y.-F. Yip, and R. A. Masut, *Appl. Phys. Lett.* **71**, 527 (1997).
- ¹⁰C. Weisbuch and B. Vinter, in *Quantum Semiconductor Structures, Fundamentals and Applications* (Academic, San Diego, 1991).
- ¹¹D. V. Lang, *J. Appl. Phys.* **45**, 3014 (1974).
- ¹²H. G. Grimmeiss and C. Ovrén, *J. Phys. E* **14**, 1032 (1981).
- ¹³N. Carlsson, T. Junno, L. Montelius, M.-E. Pistol, L. Samuelson, and W. Seifert, *J. Cryst. Growth* **191**, 347 (1998).
- ¹⁴S. K. Zhang, H. J. Zhu, F. Lu, Z. M. Jiang, and Xun Wang, *Phys. Rev. Lett.* **15**, 3340 (1998).
- ¹⁵G. J. Rees, H. G. Grimmeiss, E. Janzén, and B. Skarstam, *J. Phys. C* **13**, 6157 (1980).
- ¹⁶J. Bourgoin and M. Lannoo, in *Point Defects in Semiconductors II* (Springer-Verlag, Berlin, 1983).
- ¹⁷R. Pässler, H. Pettersson, and H. G. Grimmeiss, *Phys. Rev. B* **55**, 4312 (1997).
- ¹⁸P. M. Mooney, *J. Appl. Phys.* **67**, R1 (1990).
- ¹⁹J. Johansson, N. Carlsson, and W. Seifert, *Physica E* **2**, 667 (1998).
- ²⁰C. E. Pryor, *Phys. Rev. B* **57**, 7190 (1998).
- ²¹Chris G. Van de Walle, *Phys. Rev. B* **39**, 1871 (1989).
- ²²J. R. Waldrop, R. W. Grant, and E. A. Kraut, *Appl. Phys. Lett.* **54**, 1878 (1989).
- ²³R. P. Schneider, Jr. and B. W. Wessels, *J. Appl. Phys.* **70**, **405** (1991).
- ²⁴D. Gershoni, H. Temkin, J. M. Vanderberg, S. N. G. Chu, R. A. Hamm, and M. B. Panish, *Phys. Rev. Lett.* **60**, 448 (1988).
- ²⁵J. J. Welser, S. Tiwari, S. Rishton, K. Y. Lee, and Y. Lee, *IEEE Electron Device Lett.* **18**, 278 (1997).
- ²⁶*Semiconductors: Physics of Group IV Elements and III-V Compounds*, edited by O. Madelung, M. Schilz, and H. Weiss, Landolt-Börnstein, Vol. 17a (Springer-Verlag, New York, 1982).
- ²⁷D. D. Nolte, W. Walukiewicz, and E. E. Haller, *Phys. Rev. Lett.* **59**, 501 (1987).
- ²⁸S. Adachi, *J. Appl. Phys.* **53**, 8775 (1982).